Functional Analysis of AP-2 α and µ2 Subunits

Alison M. Motley,* Nicola Berg,† Marcus J. Taylor,‡ Daniela A. Sahlender, Jennifer Hirst, David J. Owen, and Margaret S. Robinson

Cambridge Institute for Medical Research, University of Cambridge, Cambridge CB2 2XY, United Kingdom

The AP-2 adaptor complex plays a key role in cargo recognition and clathrin-coated vesicle formation at the plasma membrane. To investigate the functions of individual binding sites and domains of the AP-2 complex in vivo, we have stably transfected HeLa cells with wild-type and mutant small interfering RNA–resistant α and µ2 subunits and then used siRNA knockdowns to deplete the endogenous proteins. Mutating the PtdIns(4,5)P2 binding site of α, the phosphorylation site of µ2, or the YXXΦ binding site of µ2 impairs AP-2 function, as assayed by transferrin uptake. In contrast, removing the C-terminal appendage domain of α, or mutating the PtdIns(4,5)P2 binding site of µ2, has no apparent effect. However, adding a C-terminal GFP tag to α renders it completely nonfunctional. These findings demonstrate that there is some functional redundancy in the binding sites of the various AP-2 subunits, because no single mutation totally abolishes function. They also help to explain why GFP-tagged AP-2 never appears to leave the plasma membrane in some live cell imaging studies. Finally, they establish a new model system that can be used both for additional structure-function analyses, and as a way of testing tagged constructs for function in vivo.

INTRODUCTION

The AP-2 adaptor complex is the major clathrin adaptor at the plasma membrane and the best characterized of all the adaptor protein (AP) complexes. Like the other AP complexes, AP-2 is a heterotetramer consisting of two large subunits (α and β2), a medium subunit (µ2), and a small subunit (σ2). The N-terminal domains of α and β2, together with µ2 and σ2, are assembled into a brick-like core or head, with the C-terminal (appendage) domains of α and β2 projecting from the core like ears, connected by flexible linkers (Owen *et al.*, 2004). The structures of the AP-2 core and appendage domains have been solved (see Figure 1), and some of the functions of the individual subunits have been established. The C-terminal appendage domains of the α and β2 subunits have been shown to interact with other proteins involved in clathrin-mediated endocytosis, forming an interconnected network. The N-terminal domain of the α subunit binds to PtdIns(4,5)P2 and has been implicated in the recruitment of AP-2 to the plasma membrane. The µ2 subunit also has a PtdIns(4,5)P2 binding site, and in addition it interacts with the internalization signal YXXΦ, which is found in cargo proteins such as the transferrin receptor (Owen *et al.*, 2004).

Both the YXXΦ binding site and the PtdIns(4,5)P2 binding site in µ2 are located in its C-terminal subdomain. In the crystalized ("inactive" conformation) AP-2 core, this domain

sits in a shallow depression formed by the other subunits, making the YXXΦ binding site inaccessible and the PtdIns(4,5)P2 binding site in the wrong orientation to interact with the membrane. This indicates that the complex undergoes a conformational change, probably favored by phosphorylation of the µ2 subunit, to flip out the µ2 C-terminal subdomain (Collins *et al.*, 2002). A µ2-specific kinase, AAK1, has been identified as one of the binding partners for the α appendage, and it has been shown to phosphorylate µ2 in a clathrin-dependent manner (Conner and Schmid, 2002). Phosphorylation of µ2 enhances the binding affinity of AP-2 for YXXΦ sorting signals by ~25-fold (Ricotta *et al.*, 2002). Thus, a working model would be one where AP-2 was initially recruited onto the plasma membrane by binding to PtdIns(4,5)P2 via its α subunit. Clathrin and AAK1 would subsequently be recruited onto the membrane-bound AP-2, and phosphorylation of the µ2 subunit would expose its binding sites for PtdIns(4,5)P2 and cargo proteins, further stabilizing the interaction of the complex with the membrane and enabling it to bind to cargo.

This model is supported by mutagenesis experiments, in particular a recent study by Höning *et al.* (2005), who used surface plasmon resonance to investigate the binding of recombinant AP-2 cores to artificial liposomes containing different phosphoinositides and sorting signals. Maximum binding was achieved using wild-type phosphorylated cores and liposomes containing both PtdIns(4,5)P2 and YXXΦ peptides. Binding was about fourfold weaker when the PtdIns(4,5)P2 binding site on the µ2 subunit was mutated or when the core was not phosphorylated and ~42-fold weaker when the YXXΦ binding site was mutated. Mutating the PtdIns(4,5)P2 binding site on the α subunit reduced the binding to background levels.

So far, all of the functional studies that have been carried out on AP-2 using mutant subunits have been done either in vitro, or in vivo in the presence of wild-type protein. We wanted to investigate the functions of AP-2 subunits in living cells by expressing mutants with little or no back-

ground from the endogenous subunits. In an earlier study, we showed that it is possible to deplete the AP-2 $\mu2$ and α subunits to undetectable levels using small interfering RNAs (siRNAs; Motley *et al.*, 2003). AP-2 depletion completely blocks clathrin-mediated endocytosis of the transferrin receptor, although interestingly we found that the epidermal growth factor (EGF) receptor and an LDL receptor chimera were still internalized normally, presumably by making use of alternative endocytic adaptors (Motley *et al.*, 2003; but see also Huang *et al.*, 2004). siRNA knockdowns can be used not only to find out what happens when a particular protein is depleted, but they can also be used to investigate other phenotypes by expressing a mutated, siRNA-resistant construct from a plasmid and then knocking down the endogenous mRNA. Here we use this strategy to analyze the functions of the PtdIns(4,5)P2 binding site and the appendage domain in the α subunit, and of the PtdIns(4,5)P2 binding site, the YXXΦ binding site, and the phosphorylation site in the $\mu2$ subunit.

MATERIALS AND METHODS

Plasmid Construction and Expression

Standard molecular biology techniques were used throughout this study (Sambrook and Russell, 2001). The $\mu2$ and αC constructs are based on ones that were originally made for in vitro liposome-binding studies (Höning *et al.*, 2005). For the present study, they were made siRNA-resistant and then cloned into pIRES-Neo2 for transfection into mammalian cells. A QuikChange Site-Directed Mutagenesis Kit (Stratagene, La Jolla, CA) was used to introduce silent mutations to prevent annealing to the siRNA. The $\mu2$ sequence was changed from AGTGGATGCCTTTCGGGTCA to AGTGGA*C*GC*T*TT*CC*G*C*GTCA, and the α sequence from GAGCATGTGCACGCTGGCCA (which hybridizes to both αA and αC) to GAG*T*ATGTG*T*ACCCT*C*GCCA. The $\mu2$ subunit had already been tagged with a myc epitope in the linker region (Höning *et al.*, 2005). To tag the α subunit, the 3' end of the mouse αC cDNA was removed using a naturally occurring ClaI site, and the comparable portion of mouse brain αA (encoding residues 639–977) was amplified by PCR and ligated to the αC cDNA. This enabled the α constructs to be detected with an antibody against a brain-specific splice variant (residues 706–727) of αA (Ball *et al.*, 1995). Two GFP-tagged α constructs were also made, using PCR to amplify the GFP so it could be ligated to the 3' end of either full-length or truncated (earless) αC. All of the PCR products and joins were sequenced to ensure that no mistakes had been introduced.

Constructs in pIRES-Neo2 were stably transfected into HeLa-M cells, and individual clones were selected by G418 resistance. Expression was monitored by Western blotting and immunofluorescence (see below). siRNA knockdowns of endogenous α and $\mu2$ were carried out as previously described (Motley *et al.*, 2003). Briefly, each 9-cm dish of cells was treated with 1 nmol siRNA on days 1 and 3, and the cells were examined on day 5.

Western Blotting and Immunofluorescence

Antibodies used for Western blotting and immunofluorescence included mouse monoclonal antibodies against the AP-2 $\alpha\alpha$ and $\mu2$ subunits (Transduction Laboratories, Lexington, KY); a rabbit polyclonal antibody against the c-myc epitope (Santa Cruz Biotechnology, Santa Cruz, CA); affinity-purified rabbit polyclonal antibodies against αC, brain αA (Ball *et al.*, 1995), and clathrin heavy chain (Simpson *et al.*, 1996); and a mouse monoclonal anti-α-adaptin, AP.6, generously provided by Frances Brodsky (UCSF). For Western blotting, incubations with mouse antibodies were followed by an incubation with rabbit anti-mouse immunoglobulin (DAKO, High Wycombe, Bucks, United Kingdom), and the blots were then probed with ^{125}I-protein A (Amersham, Newcastle upon Tyne, United Kingdom). Cell homogenates were prepared by scraping up the cells in SDS-PAGE sample buffer, boiling, and then sonicating. To separate supernatants and pellets, cells in dishes were rinsed with buffer A (0.1 M MES, pH 6.5, 0.2 mM EGTA, 0.5 mM MgCl$_2$, 0.02% NaN$_3$, 0.2 mM AEBSF), frozen in liquid nitrogen, scraped, homogenized with a glass pestle, and centrifuged at 50,000 rpm for 30 min in a Beckman TLA100.4 rotor (Fullerton, CA). The pellet was then made up to the same volume as the supernatant, and both were boiled in SDS-PAGE sample buffer. For immunofluorescence, cells were fixed with methanol for 5 min at 4°C, followed by acetone for 30 s at 4°C, before being incubated with primary antibodies. Secondary antibodies were purchased from Molecular Probes (Eugene, OR). Cells were viewed using a Zeiss Axiophot fluorescence microscope (Thornwood, NY) equipped with a CCD camera (Princeton Scientific Instruments, Monmouth Junction, NJ), and photographs were recorded using IP Labs software (Madison, WI) and then moved into Adobe Photoshop (San Jose, CA).

Assays for Transferrin Uptake

The biochemical assays for transferrin uptake were performed as previously described (Motley *et al.*, 2003). Briefly, cells in 35-mm dishes were incubated on a rocker for 30 min at 4°C in 0.6 ml serum-free medium containing ^{125}I-transferrin (Perkin-Elmer Cetus, Boston, MA) at a concentration of 500 nCi/ml and then washed. The surface counts were collected for the zero time point by incubating the cells for 5 min at 4°C with ice-cold acid wash (0.2 M acetic acid, 0.5 M NaCl). The other dishes were incubated with 1.5 ml prewarmed medium at 37°C for various times, and then endocytosis was stopped by placing the cells on ice, medium was harvested, and label associated with the cell surface was collected by acid wash, as above. The intracellular fraction was collected by extracting the cells with 1 M NaOH, and the radioactivity in the medium, acid wash, and NaOH extract was quantified using a gamma counter (Nuclear Enterprises, Edinburgh, Scotland).

Transferrin uptake was also assayed using fluorescence microscopy and flow cytometry. Cells were transiently transfected with the appropriate construct and examined after 3 d. For some experiments, the transfections were carried out on siRNA-treated cells. Knockdowns were done on day 1 and day 3, the transfection on day 2, and the assays on day 5. For all transferrin uptake experiments, the cells were first incubated for 30 min at 37°C in serum-free medium. For fluorescence microscopy, the cells were then incubated with Alexa Fluor 594–conjugated transferrin (Molecular Probes) for 10 min at 37°C, washed, fixed, and labeled as above. For flow cytometry, the cells were trypsinized, incubated for 5 min with Alexa Fluor 633–conjugated transferrin (Molecular Probes) for 5 min at 4°C, then shifted to 37°C, and incubated for a further 10 min. The cells were then pelleted, washed, acid-washed twice using 0.1 M glycine, 150 mM NaCl, pH 3, and resuspended in PBS containing 1% BSA. Flow cytometric data were acquired using a two-laser, four-color FACSCalibur flow cytometer (Becton Dickinson, Oxford, United Kingdom). Data analysis was done using CELLQuest (Becton Dickinson) and FCSPress 1.4.K software (www.fcspress.com), and the geomean was used to compare and plot data.

GFP-expressing Cells

Cells expressing αC conjugated to GFP and depleted of endogenous α were fed Alexa Fluor 598–labeled transferrin (Molecular Probes) for 30 min at 37°C, fixed with 3.7% paraformaldehyde for 15 min, and photographed as above. For fluorescence recovery after photobleaching (FRAP) experiments, the cells were examined in a Zeiss LSM510 confocal microscope, and the region of interest was bleached with a 488-nm laser at 100%. Fluorescence intensity in this region, both before and after bleaching, was measured using Zeiss LSM software, version 3.0.

Electron Microscopy

Cells to be used for electron microscopy (EM) were first incubated with mouse anti-transferrin receptor B3/25 conjugated to 10-nm gold, a kind gift from Colin Hopkins (Imperial College, London), for 30 min at 37°C. They were then fixed in tissue culture dishes and prepared for EM as previously described (Motley *et al.*, 2003). Ultrathin sections were cut using a diamond knife, collected onto formvar/carbon-coated EM grids, and stained with uranyl acetate and lead citrate. The sections were observed in a Philips CM 100 transmission electron microscope (Philips Electron Optics, Cambridge, United Kingdom) at an operating voltage of 80 kV. Micrographs were taken of cells sectioned perpendicular to the plasma membrane, and coated pits were scored as either shallow (up to hemispherical) or deeply invaginated. The raw data were as follows: for the control cells, 78 shallow pits and 59 deeply invaginated pits and for the α-GFP–expressing cells that had been depleted of endogenous α, 43 shallow pits and 46 deeply invaginated pits.

RESULTS

α Constructs

To examine the phenotypes of the α mutants, we first generated stably transfected HeLa cell lines expressing α constructs that had been tagged and made siRNA-resistant by introducing silent mutations (the siRNA is directed against a sequence that is 100% identical in the αA and αC genes). Tagging was achieved by constructing a chimera between αC and αA, which includes a brain-specific insert in the flexible linker of αA that acts as an epitope. Three constructs were made: one that was otherwise wild-type; a PtdIns(4,5)P2-binding mutant, K57E/Y58E; and an earless mutant, with a stop codon at position 745 (Figures 1 and 2A). Clonal cell lines were selected and divided into two sets of dishes, half of which were treated with the α siRNA. Expression of endogenous and transfected α was then assayed by Western blotting.
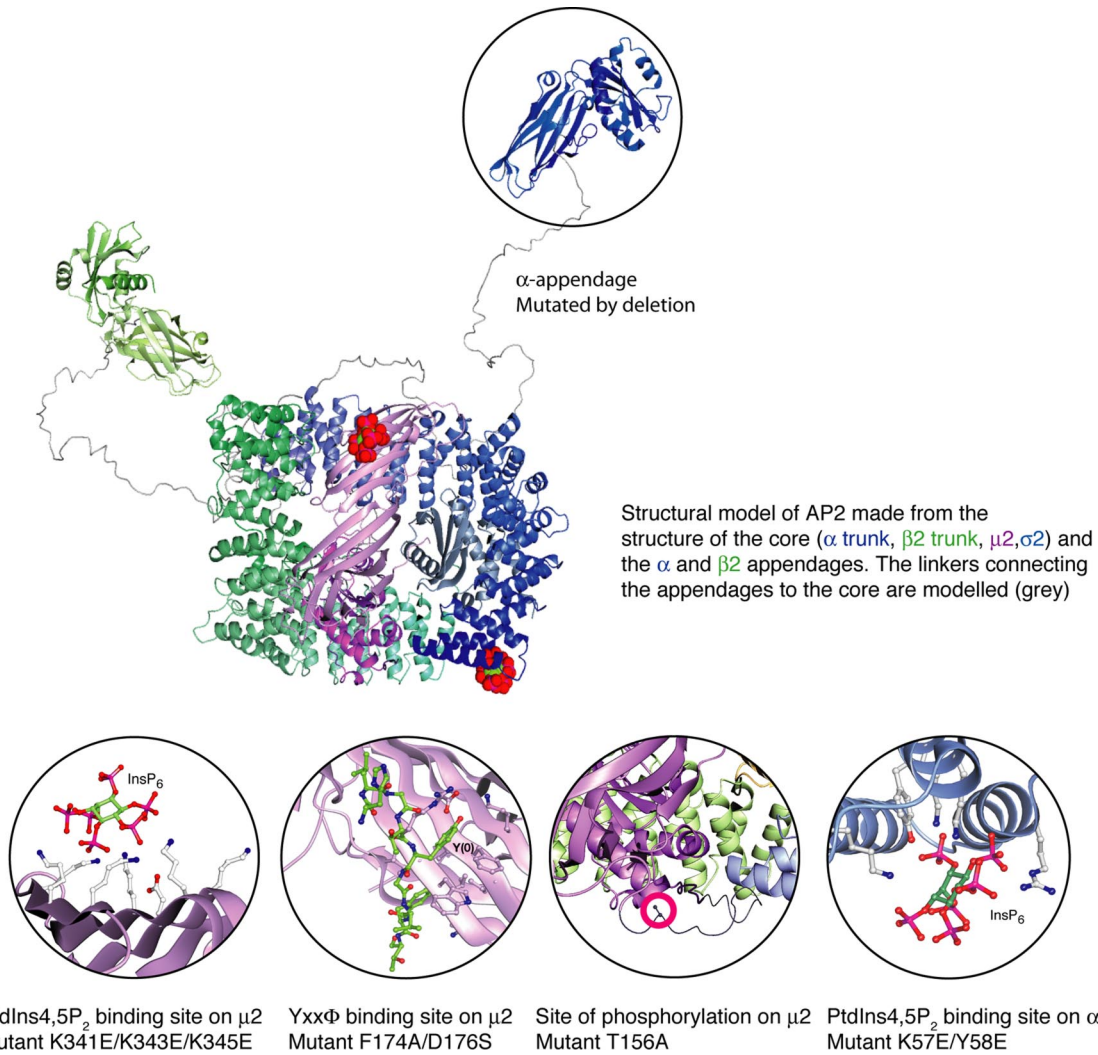
α-appendage
Mutated by deletion

Structural model of AP2 made from the
structure of the core (α trunk, β2 trunk, μ2,σ2) and
the α and β2 appendages. The linkers connecting
the appendages to the core are modelled (grey)

PtdIns4,5P$_2$ binding site on μ2
Mutant K341E/K343E/K345E

YxxΦ binding site on μ2
Mutant F174A/D176S

Site of phosphorylation on μ2
Mutant T156A

PtdIns4,5P$_2$ binding site on α
Mutant K57E/Y58E

Figure 1. Structure of the AP-2 complex and some of its binding partners, based on the x-ray crystallography data of Collins *et al.* (2002) and Owen and Evans (1998). Residues that were mutated in the present study are indicated.

Figure 2B shows blots of equal protein loadings of cells expressing the tagged α constructs, as well as control cells (i.e., cells expressing only endogenous α). The blots were probed with two different anti-α antibodies: an antibody against αA that does not cross-react with αC and an antibody against αC that does not cross-react with αA but that does react with the constructs. Labeling with the αA-specific antibody shows that the endogenous protein disappears upon knockdown. Endogenous αA is also reduced in cells expressing the various constructs, even without siRNA treatment, suggesting that when excessive amounts of α are produced, much of the endogenous αA gets degraded. Labeling with the αC-specific antibody also shows that the endogenous protein disappears upon knockdown. However, the transfected protein, which is clearly getting expressed at much higher levels than endogenous αC, does not appear to affect the expression level of the endogenous protein, indicating that the expression levels of αA and αC are regulated differently.

We also probed the blots with an antibody against the AP-2 μ2 subunit and (as a loading control) with an antibody against clathrin heavy chain (CHC). As we have previously shown (Motley *et al.,* 2003), knocking down α causes a decrease in the amount of μ2, presumably because the μ2 is unstable when it is unable to be incorporated into a heterotetrameric complex. However, overexpressing the α constructs has little or no effect on μ2 expression levels, indicating that μ2 is not up-regulated and that the total amount of AP-2 complex is similar in control cells and those expressing the various constructs.

Figure 3 shows cells expressing the three α constructs, depleted of endogenous α and labeled with a brain-specific antibody that only recognizes the transfected protein. All three constructs look essentially normal, localizing to multiple plasma membrane–associated spots with relatively little cytoplasmic fluorescence. Because the μ2 subunit is not up-regulated and because the α subunit does not localize to membranes in the absence of μ2 (Motley *et al.,* 2003; see also Figure 6B), we suspect that the excess α gets washed away during the methanol/acetone fixation/permeabilization procedure. There may be slightly smaller puncta in cells expressing the PtdIns(4,5)P2-binding mutant. However, the labeling clearly indicates that AP-2 constructs containing the PtdIns(4,5)P2-binding α mutant are able to be recruited onto the plasma membrane, albeit possibly less efficiently, even
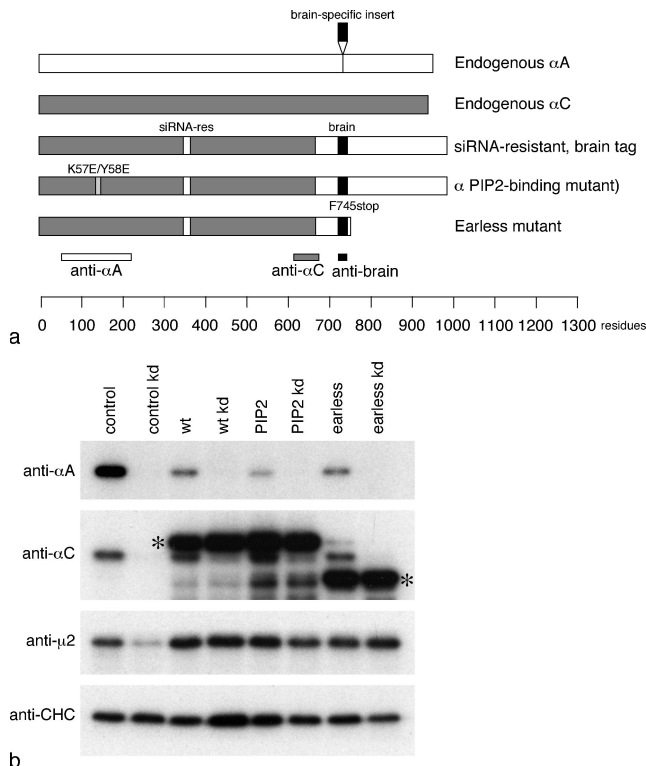
Figure 2. Brain-tagged α constructs used in this study. (a) Schematic diagram of the three brain-tagged constructs. (b) Homogenates of control cells and cells stably transfected with the brain-tagged α constructs, either with or without treatment with an siRNA to deplete endogenous α, were subjected to SDS-PAGE and blotted, and the blots were probed with antibodies against αA, αC, μ2, or clathrin heavy chain (CHC) as a loading control. Labeling with the αA antibody, which does not cross-react with the constructs, shows that endogenous αA disappears upon knockdown and is also reduced in cells expressing large amounts of construct. Labeling with the αC antibody, which recognizes both the endogenous protein and the constructs, shows that the endogenous protein disappears upon knockdown, whereas the constructs (asterisks) do not. Expression of μ2 is reduced in the control knockdown because the protein is unstable in the absence of the other AP-2 subunits; however, it does not appear to be up-regulated in the cells that overexpress the various α constructs.

though in vitro the cores of such complexes showed no detectable binding to liposomes (Höning *et al.*, 2005).

We next investigated whether the AP-2 complexes assembled from transfected α subunits were functional by assay-
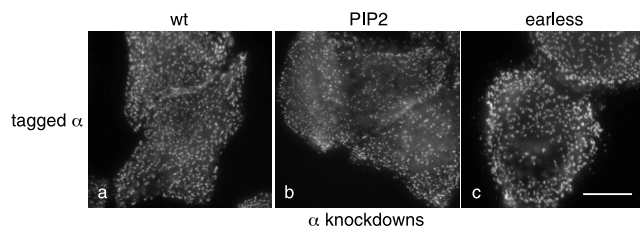

Figure 3. Cells were stably transfected with the indicated brain-tagged α constructs and then depleted of endogenous α and labeled with an antibody against the brain epitope. All three constructs have a punctate distribution, although there may be slightly less of the PtdIns(4,5)P2 binding mutant associated with the plasma membrane. Scale bar, 20 μm.

ing their ability to support receptor-mediated endocytosis of transferrin in siRNA-treated cells. Each cell line was tested in triplicate experiments carried out on different days, and both positive and negative controls were included (i.e., completely untreated cells and siRNA-treated nontransfected cells, respectively). Figure 4a shows that wild-type α (i.e., tagged and siRNA-resistant only) gave full rescue and was indistinguishable from the positive control. Surprisingly, the earless mutant also gave full rescue, and the PtdIns(4,5)P2-binding mutant gave partial rescue. This is presumably not a reflection of the efficiency of the knockdown, because by Western blotting endogenous α was undetectable (see Figure 2B). Thus, the two AP-2 complexes containing mutated α subunits were both either fully or partially functional.

To ensure that the results we obtained using stably transfected cells were not affected by events that might have occurred during the generation of the cell lines (e.g., overexpression of other proteins to compensate for defective α subunits), we also investigated transferrin uptake in transiently transfected cells. The cells were transfected with either the wild-type α construct or the PtdIns(4,5)P2-binding mutant and examined after 3 d. In cells that had not been depleted of endogenous α, uptake of fluorescent transferrin did not appear to be affected by either of the two constructs (Figure 4, b–e). When we transfected the cells during the course of an siRNA knockdown, we found that both constructs were able to rescue the phenotype to some extent and that the wild-type construct generally gave better rescue than the PtdIns(4,5)P2-binding mutant (Figure 4, f–i), consistent with the biochemical data on stably transfected cells. However, even in the cells expressing the wild-type construct, uptake appeared diminished when compared with untreated cells or with stably transfected siRNA-treated cells, suggesting that 3 d is not long enough for full incorporation of the α constructs into functional AP-2 complexes.

μ2 Constructs

The μ2 constructs were tagged with a myc epitope inserted into the linker between the N- and C-terminal subdomains. Again, silent mutations were introduced to make the constructs siRNA-resistant. Four constructs were made: one that was otherwise wild-type; a PtdIns(4,5)P2-binding mutant, K341E/K343E/K345E; a YXXΦ-binding mutant, F174A/D176S; and a phosphorylation mutant, T156A (Figures 1 and 5A).

Western blots of cells transfected with the various μ2 constructs were probed with an antibody that recognizes both endogenous and tagged μ2, with anti-myc, or with anti-CHC as a loading control (see Figure 9B). Labeling with the μ2 antibody shows a single band in untreated control cells, which disappears upon knockdown. This band shifts upward and becomes broader in cells transfected with the various constructs because of the coexpression of myc-tagged μ2, which runs at a slightly higher apparent molecular weight. Knocking down endogenous μ2 sharpens the bands in the transfected cells by causing the lower molecular weight component to disappear. Labeling with anti-myc shows that the constructs are not depleted by the knockdown. Interestingly, the cells appear to be able to regulate their levels of μ2 so that the total amount of μ2 (i.e., endogenous plus construct) remains essentially constant, presumably by degrading any excess protein that is not incorporated into AP-2 complexes. A similar phenomenon was reported by Nesterov *et al.* (1999), who used COS-1 cells stably transfected with tagged μ2.

Figure 6 shows immunofluorescence labeling of the cell lines expressing the various μ2 constructs, together with
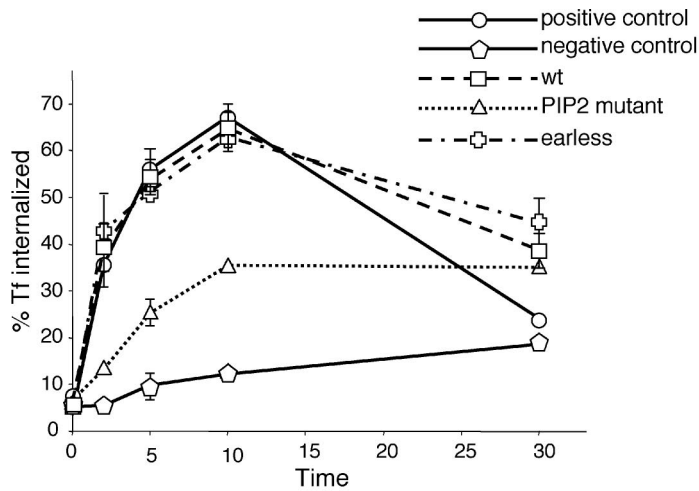
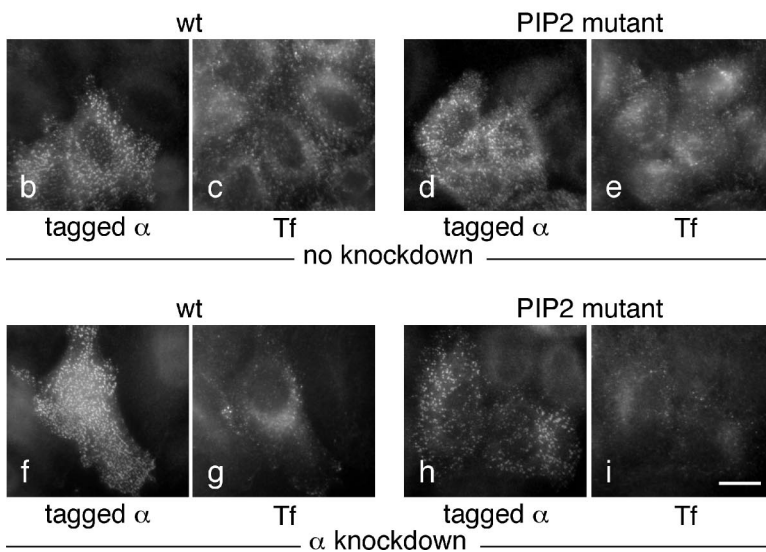**a** α knockdown, brain-tagged α rescue

Figure 4. Receptor-mediated endocytosis of transferrin in cells expressing the brain-tagged α constructs. (a) Cells were allowed to bind ^{125}I-labeled transferrin at 4°C and then shifted to 37°C for the indicated length of time, after which the medium was harvested, ligand remaining on the cell surface was released with an acid wash, the cells were solubilized with NaOH, and all three fractions were quantified and expressed as % total counts. The graph shows the percentage of the total counts recovered in the NaOH extract (i.e., internalized transferrin). The cells used for the positive control were neither transfected nor treated with siRNA; the cells used for the negative control were treated with siRNA only. All other cells were stable cell lines expressing brain-tagged α constructs, which were depleted of endogenous α using siRNA. The wild-type and earless constructs fully rescue the knockdown phenotype; the PtdIns(4,5)P2 binding mutant gives partial rescue. (b–i) Cells were transiently with either the wild-type α construct (b, c, f, and g) or the PtdIns(4,5)P2 binding mutant (d, e, h, and i), either with (f–i) or without (b–e) concurrently knocking down endogenous α. Alexa Fluor 594–conjugated transferrin was added to the cells for 10 min at 37°C. Neither construct has a dominant negative effect, and they both appear to give at least partial rescue, consistent with the biochemical data on stably transfected cells shown in a. Scale bar, 20 μm.

control (nontransfected) cells. Control cells labeled with an antibody against the α subunit show the characteristic punctate pattern (a), which becomes diffuse and cytosolic after μ2 knockdown (b). The cells in c–j were all stably transfected with myc-tagged μ2 constructs and then depleted of endogenous μ2 and labeled with either anti-myc (c–f) or anti-α (g–j). Although the myc antibody produces a higher background than the α antibody, the labeling looks essentially normal in every cell line, indicating that AP-2 complexes containing the constructs are able to be recruited efficiently onto the plasma membrane, even though all three mutants have been shown to be impaired in their ability to be recruited onto liposomes (Höning *et al.*, 2005).

Transferrin uptake assays (Figure 7) showed that both the wild-type μ2 construct and the PtdIns(4,5)P2-binding mutant gave full rescue, even though a similar mutant has been reported to have a dominant negative effect when transiently transfected into CHO cells (Rohde *et al.*, 2002). Both of the other two mutants, the YXXΦ-binding mutant and the phosphorylation mutant, gave partial rescue.

GFP-tagged α Subunit

All of the constructs described so far were found to be at least partially functional, even when we disrupted various

binding sites. Interestingly, however, the first tagged α construct that we made behaved very differently. Others have inserted GFP tags at either the N terminus or the C terminus of α for live cell imaging studies (Rappoport *et al.*, 2003; Keyel *et al.*, 2004; Rappoport *et al.*, 2005), and initially we inserted a C-terminal GFP tag (Figure 8A). Although we were unable to isolate a completely homogeneous population of cells, we generated cell lines in which ~60% of the cells were expressing tagged α, and Western blotting showed selective disappearance of endogenous αA and αC after siRNA knockdown (Figure 8B). As others have reported, C-terminally GFP-tagged α has the same punctate pattern as endogenous α (see Figure 10A). However, when we carried out transferrin uptake assays (Figure 9A), we found that GFP-tagged α was unable to rescue the phenotype of siRNA-treated cells. This is in contrast to our α and μ2 mutants: even constructs that were impaired in their ability to bind to important partners were still at least partially functional when we assayed transferrin uptake, whereas uptake in cells expressing GFP-tagged α was not significantly different from the negative control.

Because the extra bulk of the GFP tag might be sterically hindering certain protein-protein interactions, we also made a construct in which the GFP tag replaced the ear domain,
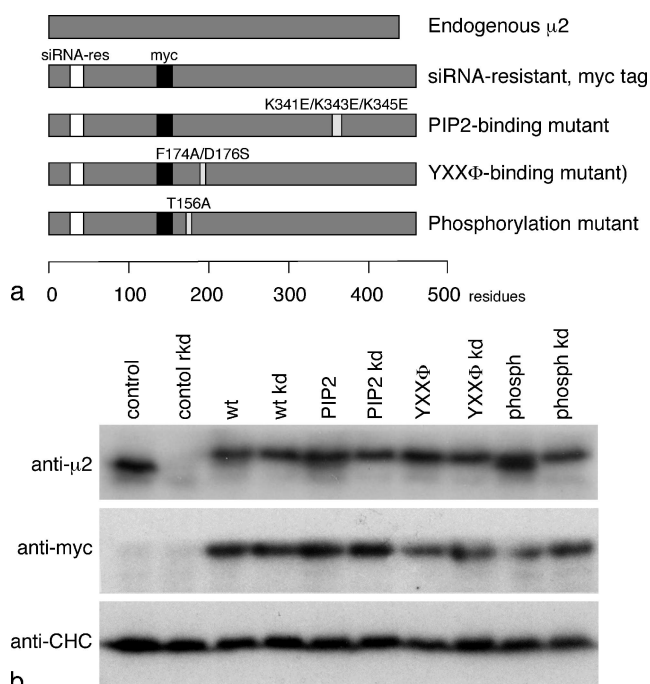
Endogenous μ2

siRNA-res   myc

siRNA-resistant, myc tag

K341E/K343E/K345E

PIP2-binding mutant

F174A/D176S

YXXΦ-binding mutant)

T156A

Phosphorylation mutant

0   100   200   300   400   500 residues

a

anti-μ2

anti-myc

anti-CHC

b

control · contol rkd · wt · wt kd · PIP2 · PIP2 kd · YXXΦ · YXXΦ kd · phosph · phosph kd

Figure 5. μ2 constructs used in this study. (a) Schematic diagram of the four constructs. (b) Homogenates of control and stably transfected cells, either with or without treatment with an siRNA to deplete endogenous μ2, were subjected to SDS-PAGE and blotted, and the blots were probed with either an antibody that recognizes both endogenous and transfected μ2, an antibody against the myc tag on the transfected μ2, or an antibody against clathrin heavy chain (CHC) as a loading control. The endogenous μ2, which runs slightly faster because it is not tagged, disappears upon knockdown, whereas the transfected, tagged μ2 is not affected.

Figure 4a shows that earless α with a suitable tag fully rescues the transferrin uptake phenotype. Thus, for reasons that are still not clear, inserting a GFP tag at the C terminus produces a nonfunctional α subunit.

Is the GFP-tagged α dominant negative, or simply "dead"? To look for possible dominant negative effects, cells were transiently transfected with α-GFP, either with or without concurrently knocking down endogenous α, and assayed after 3 d for uptake of Alexa Fluor 633–conjugated transferrin by flow cytometry. Figure 9B shows that in the absence of siRNA knockdown, cells expressing α-GFP are not impaired in their ability to endocytose transferrin, when compared with nontransfected controls. When we knocked down endogenous α, uptake was reduced by ~10-fold, whether or not the cells were expressing the α-GFP construct. Therefore, at least with the level of expression and incorporation seen in transiently transfected cells, the construct appears to be nonfunctional (consistent with our biochemical assay) but not inhibitory. However, it is possible that at higher expression levels, or with more time to incorporate into AP-2 complexes, the GFP-tagged construct would be able to outcompete endogenous α and act as a dominant negative.

Why are cells expressing GFP-tagged α unable to internalize transferrin? Initially we suspected that coated pits assembled from this construct might be unable to sequester transferrin receptors. However, when we incubated the siRNA-treated cells with Alexa Fluor 594–conjugated transferrin for 30 min at 37°C, we found that the transferrin had a punctate pattern that coincided with the α-GFP labeling, indicating that the transferrin receptor is able to enter the coated pits but the pits are unable to pinch off as coated vesicles (Figure 10, a and b). Another possibility was that the GFP-tagged AP-2 might be getting trapped on the membrane and unable to participate in the normal cycle of coat assembly and disassembly. However, when we carried out FRAP experiments (Figure 10, c–f), we found that most of the signal was recovered, with the same pattern of spots reappearing, indicating that there is exchange between
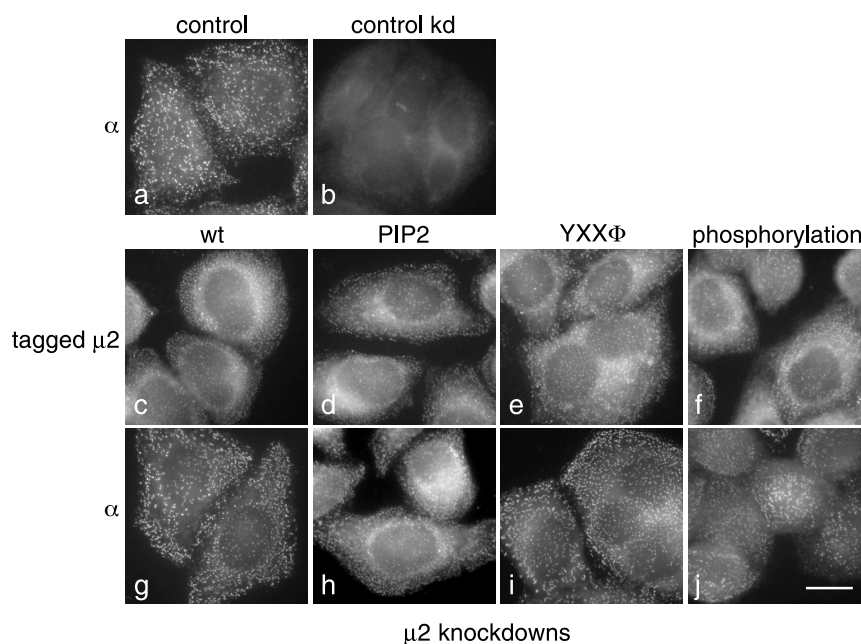
which was similar in size to endogenous α (Figure 8A). Again, however, transferrin uptake was not significantly different from the negative control (Figure 9A), even though

control   control kd

α

a   b

wt   PIP2   YXXΦ   phosphorylation

tagged μ2

c   d   e   f

α

g   h   i   j

μ2 knockdowns

Figure 6. Immunofluorescence localization of AP-2 complexes containing the μ2 constructs. (a and b) Nontransfected cells were labeled with an antibody against the α subunit, either under control conditions (a) or after first depleting μ2 (b). The normal punctate pattern completely disappears upon μ2 knockdown. (c–j) Cells were stably transfected with siRNA-resistant, myc-tagged μ2 constructs and then depleted of endogenous μ2. The constructs were as follows: wild-type (c and g), PtdIns(4,5)P2-binding mutant (d and h), YXXΦ-binding mutant (e and i), and phosphorylation mutant (f and j). The cells were labeled either with anti-myc (c–f) or with anti-α (g–j). Both proteins show the punctate pattern characteristic of AP-2. Scale bar, 20 μm.
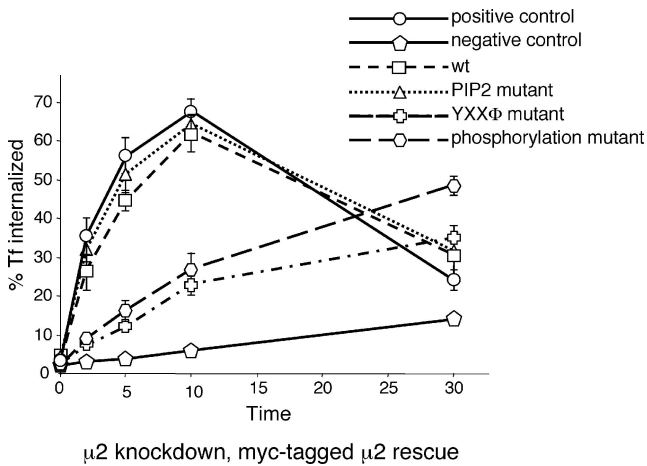
μ2 knockdown, myc-tagged μ2 rescue

Figure 7. Receptor-mediated endocytosis of transferrin in cells expressing μ2 constructs. Cells were treated as in Figure 4; the graph shows the percentage of the total counts that were internalized. The wild-type and PtdIns(4,5)P2 mutant constructs fully rescue the knockdown phenotype; the YXXΦ and phosphorylation mutants give partial rescue.

membrane-bound and cytosolic AP-2 containing α-GFP in the coated pits.

What do the coated pits look like? To examine the ultrastructure of the pits, we carried out EM on cells expressing α-GFP and depleted of endogenous α, as well as on control cells, which had been incubated for 30 min at 37°C with anti-transferrin receptor coupled to colloidal gold. The coated pits looked very similar in the two populations of cells, although the block in endocytosis in the cells express-
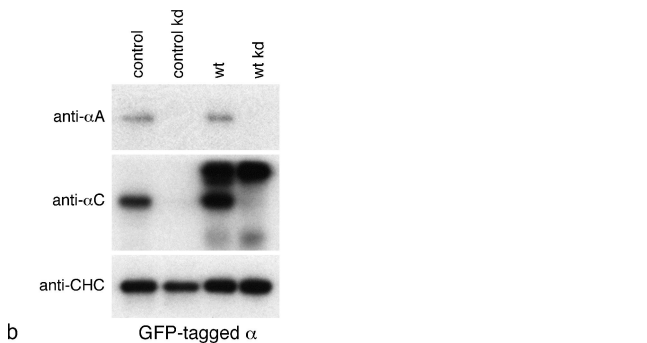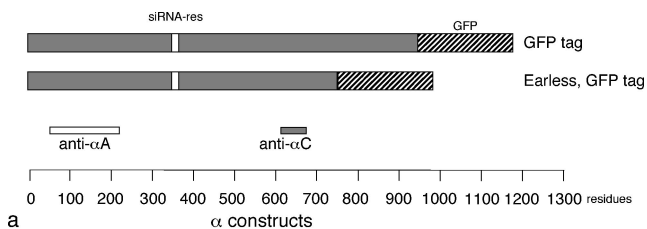

Figure 8. GFP-tagged α constructs used in this study. (a) Schematic diagram of the two GFP-tagged constructs. (b) Homogenates of control cells and cells stably transfected with the GFP-tagged α construct, either with or without treatment with an siRNA to deplete endogenous α, were subjected to SDS-PAGE and blotted, and the blots were probed with antibodies against αA, αC, or clathrin heavy chain. Endogenous αA and αC disappear upon knockdown; the construct does not.
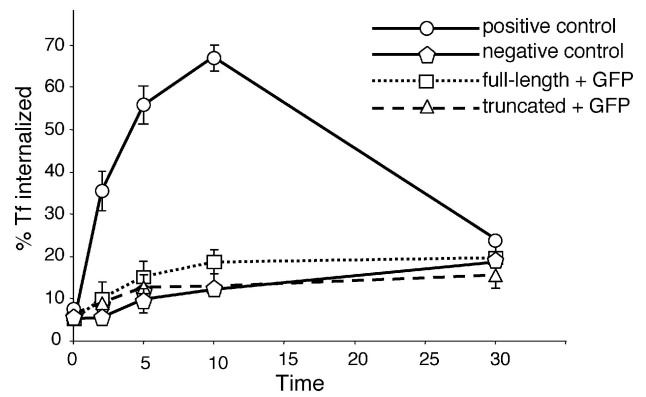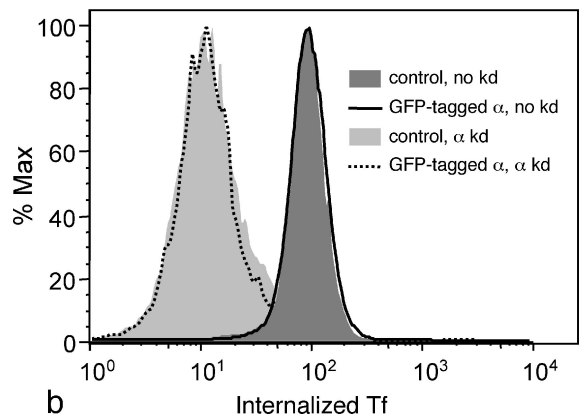

a α knockdown, GFP-tagged α rescue

b

Figure 9. Receptor-mediated endocytosis of transferrin in cells expressing GFP-tagged α constructs. (a) Cells were treated as in Figures 4 and 7; the graph shows the percentage of the total counts that were internalized. The GFP-tagged constructs fail to rescue the knockdown phenotype. (b) Cells were transiently with GFP-tagged α, either with or without concurrently knocking down endogenous α. The cells were allowed to internalize Alexa Fluor 633–conjugated transferrin for 10 min at 37°C and then any transferrin remaining on the cell surface was washed off at low pH, and the cells were analyzed by flow cytometry. Expression of the GFP-tagged construct does not appear to have a dominant negative effect, nor does it rescue the knockdown phenotype, consistent with the biochemical data on stably transfected cells.

ing GFP-tagged α was evident from the accumulation of gold particles in the pits and relative absence of gold particles in endosomes (Figure 10, g–j). To look for subtle differences in the morphology of the coated pits, we scored all of the coated structures associated with the plasma membrane as either shallow pits (up to hemispherical in shape; e.g., Figure 10, g and h) or deeply invaginated pits (e.g., Figure 10, i and j). Although there was a slightly higher percentage of deeply invaginated pits in the cells expressing only GFP-tagged α (52% compared with 43% in control cells), this difference may not be significant. This is in contrast to other constructs and reagents that interfere with clathrin-mediated endocytosis. For instance, cells expressing dynamin mutants accumulate a very high percentage of deeply invaginated pits, often with aberrantly long necks (Damke *et al.,* 2001). Chemical treatments have been shown either to flatten clathrin-coated pits or to cause microcages to form around them (Heuser, 1989; Heuser and Anderson, 1989). The relatively normal appearance of the pits in cells expressing α-GFP, together with the behavior of the α-GFP construct in
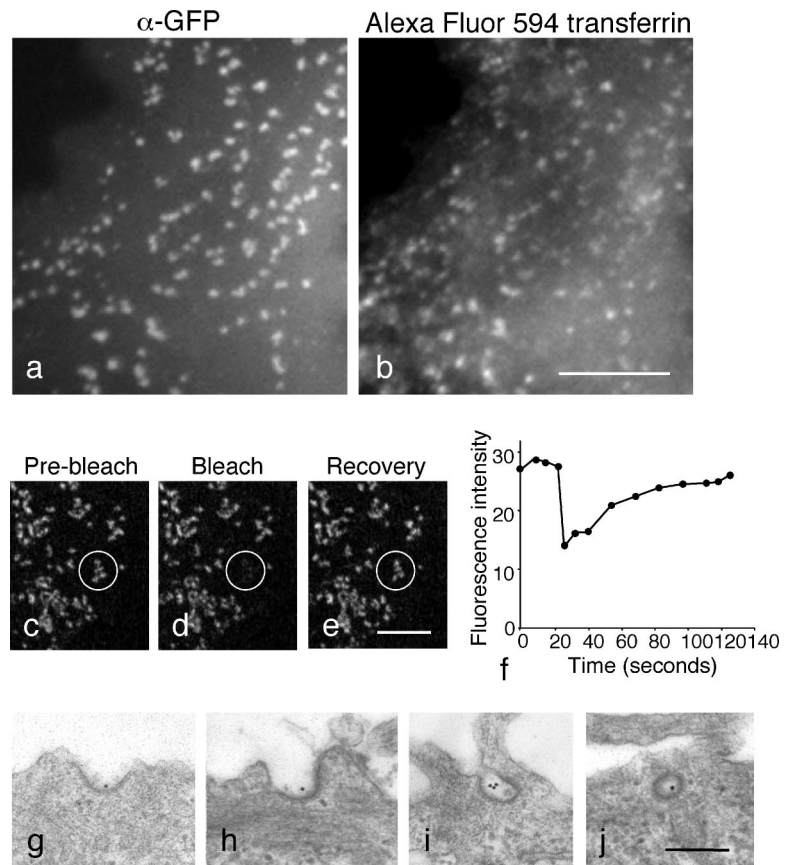
α-GFP   Alexa Fluor 594 transferrin

Figure 10. Localization and behavior of GFP-tagged α in cells depleted of endogenous α. (a and b) Cells were incubated with Alexa Fluor 594–conjugated transferrin for 30 min at 37°C. Although the transferrin stays on the cell surface, it is able to get into coated pits where it colocalizes with α-GFP. Scale bar, 10 μm. (c–f) Fluorescence recovery after photobleaching (FRAP). A spot was bleached and fluorescence recovery was monitored. The same pattern of dots returns after 1–2 min, indicating that there is exchange between membrane-bound and cytosolic-tagged AP-2. Scale bar, 10 μm. (g–j) Electron micrographs of cells expressing GFP-tagged α and depleted of endogenous α incubated for 30 min at 37° with gold-conjugated anti-transferrin receptor. Coated pits range from shallow (g and h) to deeply invaginated (i and j), indicating that their morphology is not affected even though they are incapable of transferrin uptake. Scale bar, 200 nm.

FRAP experiments, suggests that the clathrin coats are still flexible and dynamic, even though the final scission event is blocked.

DISCUSSION

By stably transfecting HeLa cells with mutated AP-2 subunits and then carrying out siRNA knockdowns, we have been able to investigate the functions of individual binding sites and domains in vivo with no detectable background from the endogenous subunits. Some of our results were as predicted, whereas others were unexpected. In particular, some amino acid substitutions that had been shown to inactivate binding sites and/or to interfere with recruitment of AP-2 cores onto membranes in vitro produced relatively mild phenotypes in vivo. In contrast, the addition of a C-terminal GFP tag to the α subunit, which we thought would be noninvasive, had a more devastating effect on the function of the AP-2 complex than any of the mutations.

Of the two α mutants that we tested, one (the PtdIns(4,5)P2-binding mutant) was partially functional and the other (the earless mutant) was fully functional. The relative effects of these two mutants are broadly in agreement with the work of Höning et al. (2005), who used entirely earless AP-2 cores for liposome binding and found that mutating the PtdIns(4,5)P2 binding site on α impaired recruitment. However, the recombinant AP-2 cores containing the PtdIns(4,5)P2-binding α mutant completely failed to be recruited onto liposomes, whereas our immunofluorescence results demonstrate that in vivo, whole AP-2 complexes containing this mutant are capable of being recruited onto the plasma membrane. This indicates that there are additional interactions taking place in the whole cell,

which were not reconstituted in the liposome system. For instance, although the liposomes contained only a single AP-2–dependent sorting signal (either YXXΦ or D/EXXXLL), the plasma membrane contains both types of sorting signals and possibly others as well. In addition, the ear domains of the α and β2 subunits interact with accessory proteins at the plasma membrane, and there is evidence that they contribute to recruitment even though they are not absolutely required (Robinson, 1993; Page and Robinson, 1995).

In an earlier study on the PtdIns(4,5)P2 binding site of the α subunit, published before the structure was solved, three lysines were mutated to glutamines (K55Q/K56Q/K57Q), and this construct was reported to be unable to recruit onto membranes and to have a dominant negative effect on transferrin uptake (Gaidarov and Keen, 1999). Our mutations (K57E/Y58E) were based on the crystal structure of the AP-2 core with a phosphoinositide head group bound to α, and they do not interfere with the assembly or stability of the recombinant AP-2 complex (Höning et al., 2005). In addition, we were able to show by circular dichroism that the overall structure of the complex is normal (unpublished observations). In contrast, the mutations made in the earlier study may have affected protein folding as well as PtdIns(4,5)P2 binding. Another difference is that in the earlier study the cells were transfected with tagged α without knocking down endogenous α, which may have reduced the signal relative to background. The dominant negative effect on transferrin uptake is consistent with our results on stably transfected cells, although we did not see any obvious differences in transferrin uptake when we looked at transiently transfected cells. Possibly the PtdIns(4,5)P2-binding mutant in the ear-

lier study was expressed at higher levels and thus competed out the endogenous protein more effectively.

We were surprised by the wild-type phenotype of the earless α mutant in the transferrin uptake assay. The α ear binds to many of the accessory proteins that contribute to clathrin-mediated endocytosis, including the $\mu 2$ kinase AAK1; the DnaJ homologue, auxilin, and the PtdIns(4,5)P2 5-phosphatase, synaptojanin, both of which are implicated in vesicle uncoating; epsin and amphiphysin, both thought to play a role in membrane curvature; and members of the AP180/CALM family, which are thought to regulate vesicle size. There are also indirect α ear binding partners such as dynamin, which facilitates vesicle scission, and intersectin, which functions as a guanine nucleotide exchange factor for Cdc42, linking the endocytic machinery with the actin cytoskeleton and associated signaling pathways (Slepnev and De Camilli, 2000). The full rescue that we obtained with earless α indicates either that these proteins are not essential for clathrin-coated vesicle (CCV) formation or that they have other ways of engaging with the machinery. The second possibility seems more likely, especially because several of these proteins have been shown to bind not only to the α ear, but also to the β2 ear, as well as to PtdIns(4,5)P2 and/or clathrin in their own right (Slepnev and De Camilli, 2000; Edeling *et al.*, 2006). It would also explain the dominant negative effects that have been reported on cells overexpressing α ear constructs (Owen *et al.*, 1999): the ear may be titrating out important binding partners and preventing them from getting incorporated into the coated pit through other interactions.

One CCV accessory protein that appears to depend on its interaction with the α ear in order to function is Numb, which was originally identified in *Drosophila* screens for genes involved in cell fate determination. A subsequent screen for additional genes with a similar mutant phenotype to *numb* turned up three alleles of the AP-2 α subunit, all with premature stop codons that truncated the protein in the middle of the ear domain (called *ada^{ear}* alleles; Berdnik *et al.*, 2002). Interestingly, homozygous *ada^{ear}* cells were completely viable, whereas an α deletion mutant (*ada^3*) had been shown in an earlier study to be embryonic lethal and was postulated to interfere with normal cell growth and function (Gonzalez-Gaitan and Jackle, 1997). Flies homozygous for a third mutant α allele, *ada^1*, with a P element insertion in the 5′ UTR and reduced expression levels, have defects mainly in synaptic vesicle recycling. However, *ada^{ear}/ada^1* heterozygotes are phenotypically normal (Berdnik *et al.*, 2002). These findings, together with our own results, indicate that earless α is completely functional for general endocytosis, and that the ear is only needed to bind a few partners, such as Numb, that carry out more specialized activities.

Of the three $\mu 2$ mutants that we tested, one (the PtdIns(4,5)P2-binding mutant) was completely functional, and the other two (the phosphorylation mutant and the YXXΦ-binding mutant) were partially functional. Again, these results are broadly in agreement with the work of Höning *et al.* (2005), who found that the PtdIns(4,5)P2-binding $\mu 2$ mutant had the mildest phenotype of all the mutants they tested in their liposome recruitment assay. However, Haucke and coworkers have reported that AP-2 complexes containing a PtdIns(4,5)P2-binding $\mu 2$ mutant fail to be recruited onto the plasma membrane and have a dominant negative effect on transferrin uptake (Rohde *et al.*, 2002). Again, one possible explanation for the discrepancy between their results and ours is that the two PtdIns(4,5)P2-binding mutants are different: our mutations (K341E, K343E, and K345E) were structurally based, whereas theirs (K345E,

K354E, and K356E) were engineered before the structure was known. Thus, it is possible that the mutant made in the earlier study may not have folded as well as our construct and/or that the localization pattern may have been affected by the presence of wild-type protein. The reported effect on clathrin-mediated endocytosis is more difficult to explain, because we find that the PtdIns(4,5)P2-binding $\mu 2$ mutant is fully capable of transferrin uptake. However, it is worth noting that in the previous study the phenotype was analyzed by fluorescence microscopy, which is less quantitative than our biochemical assay. In addition, the three mutations made in the earlier study cover more of the surface of the $\mu 2$ C-terminal subdomain, and they might have affected binding to other, as yet unidentified partner(s) as well as to PtdIns(4,5)P2.

Unlike the PtdIns(4,5)P2-binding $\mu 2$ mutant, neither the phosphorylation mutant nor the YXXΦ-binding mutant had a wild-type phenotype. However, both were at least partially functional. Höning *et al.* (2005) have shown that $\mu 2$ phosphorylation contributes to the binding of AP-2 to YXXΦ-containing liposomes but is not absolutely essential. This indicates that the conformational change that exposes the YXXΦ binding site on the $\mu 2$ subunit is favored but is not driven by phosphorylation, which is entirely consistent with our own results. Our study also agrees with an article by Olusanya *et al.* (2001) on the role of $\mu 2$ phosphorylation in vivo, in which tagged wild-type or T156A $\mu 2$ were transiently transfected into cells. Both wild-type and mutant constructs were able to be recruited onto the plasma membrane, but the mutant construct appeared to have a dominant negative effect on the uptake of fluorescent transferrin.

It is harder to explain why the YXXΦ binding mutant was partially functional. The F174A/D176S mutation reduces the affinity of the $\mu 2$ C-terminal domain for YXXΦ peptides to background levels as assayed by fluorimetry (unpublished data), and the binding of AP-2 complexes containing this mutant to YXXΦ-containing liposomes is not significantly different from binding to liposomes alone (Höning *et al.*, 2005). Possibly the very weak binding of the mutant $\mu 2$ to the transferrin receptor is still sufficient in vivo for a limited amount of clathrin-mediated endocytosis. Alternatively, because even the most efficient knockdown does not get rid of 100% of its target, it is possible that the trace amounts of AP-2 containing wild-type $\mu 2$ can function more effectively when the cell has a normal number of clathrin-coated pits. We have previously shown that depleting AP-2 reduces the number of coated pits by ~12-fold (Motley *et al.*, 2003), and although we found that EGF was still internalized with normal kinetics in these cells, Huang *et al.* (2004) subsequently showed that the rate of EGF uptake in AP-2–depleted cells depends very much on the experimental conditions. If the cells are allowed to prebind EGF at 4°C and then are warmed to 37°C, the rate of internalization is the same as in wild-type cells. However, if the cells are incubated in the continuous presence of EGF at 37°, uptake is significantly slower. Their explanation for these results was that at 4°C, the EGF receptor is able to be captured efficiently by the few pits remaining in AP-2–depleted cells. However, under steady state conditions, EGF gets in more slowly because there are fewer entry points. Thus, there is a precedent for AP-2 promoting cargo uptake by acting as a template for clathrin-coated pit formation, without actually sorting the cargo directly.

Perhaps our most surprising result was the deleterious effect of the GFP tag on the α subunit. We initially inserted a GFP tag into our α constructs as a way of localizing them, because GFP-tagged α had been previously used for live cell imaging studies (Rappoport *et al.*, 2003; Keyel *et al.*, 2004;

Rappoport *et al.,* 2005). Some of the results of these studies have been puzzling, and our data may help to explain them. Both GFP-tagged α and dsRed-tagged clathrin colocalize in fluorescent spots associated with the plasma membrane. However, the α spots appear static, whereas the clathrin spots can move parallel to the plane of the plasma membrane and then disappear. These events have been interpreted as CCV budding, movement, and uncoating. Because the GFP-α is not incorporated into the moving spots, it has been hypothesized that AP-2 is somehow swept aside as the vesicle buds (Rappoport *et al.,* 2003, 2005). Our results suggest an alternative interpretation. The behavior of the GFP-tagged α in the live cell imaging studies is consistent with our discovery that it is unable to support clathrin-mediated endocytosis. Because the live cell experiments were done without knocking down endogenous α, we propose that the moving and disappearing clathrin spots do in fact contain AP-2, but only unlabeled AP-2. This would explain how the cell is able to keep the clathrin attached to the membrane and the transferrin receptors in place as the vesicle buds, which would be difficult to achieve if there were no AP-2 to act as an adaptor. However, it is possible that GFP tags are more innocuous when placed on other AP-2 subunits. Ehrlich *et al.* (2004) have labeled the $\sigma2$ subunit with GFP and found that it colocalized not only with static clathrin spots, but also with those that move and disappear. In addition, AP-2 complexes containing GFP-tagged α expressed at relatively low levels may be better able to equilibrate with AP-2 complexes containing endogenous α and become incorporated into CCVs. In the two studies by Rappoport *et al.,* the tagged α was expressed for at least 40 h before imaging. However, when Keyel *et al.* (2004) expressed a C-terminally GFP-tagged α construct for only 18 h, they saw codisappearance of AP-2 and clathrin spots. Precisely why GFP would have this effect is still not clear, but it has been noted that GFP has a tendency to dimerize at high concentrations, especially when the protein is confined to two dimensions (Zacharias *et al.,* 2002). AP-2 in clathrin-coated pits is very highly concentrated in the plane of the plasma membrane, and if the tagged complex is forming dimers, this interaction might interfere with the normal dynamics of the CCV cycle. GFP and RFP variants have been engineered in which the tendency to dimerize has been suppressed (Zacharias *et al.,* 2002), and these reporters may be more suitable for studies on clathrin-mediated endocytosis.

Thus, the approach of stably transfecting cells with siRNA-resistant constructs and then knocking down the endogenous protein can be used not only to investigate mutant phenotypes, but also to test tagged constructs for functionality. By using homogeneous populations of cells, it is possible to carry out biochemical assays, which are not only more quantitative than microscopy-based assays, but which also show up differences that otherwise might be missed. For instance, when we first investigated the phenotypes of our constructs in siRNA-treated cells, we mixed together expressing and nonexpressing cells, fed them fluorescent transferrin, and examined them by immunofluorescence microscopy. It was clear that cells expressing even mutant constructs were taking up more transferrin than their nonexpressing neighbors (see Figure 4, f–i), leading us initially to assume that all of the mutants were completely functional. It was not until we looked at the internalization of ^{125}I-transferrin that we were able to see clear differences in the kinetics of uptake.

In organisms like yeast, it has long been relatively straightforward to replace wild-type genes with mutated ones, but until recently in mammalian cells one has had to rely on overexpression, usually after transient transfection, to try to compete out most of the endogenous protein. With the advent of siRNA technology, it is now possible to investigate the phenotype of cells expressing almost exclusively mutant genes at moderate levels. Thus, the strategy adopted in the present study should help to facilitate structure–function analyses of other mammalian proteins in addition to AP-2 subunits.

REFERENCES

Ball, C. L., Hunt, S. P., and Robinson, M. S. (1995). Expression and localisation of α-adaptin isoforms. J. Cell Sci. *108,* 2865–2875.

Berdnik, D., Torok, T., Gonzalez-Gaitan, M., and Knoblich, J. A. (2002). The endocytic protein alpha-adaptin is required for Numb-mediated asymmetric cell division in *Drosophila.* Dev. Cell *3,* 221–231.

Collins, B. M., McCoy, A. J., Kent, H. M., Evans, P. R., and Owen, D J. (2002). Molecular architecture and functional model of the endocytic AP2 complex. Cell *109,* 523–535.

Conner, S. D., and Schmid, S. L. (2002). Identification of an adaptor-associated kinase, AAK1, as a regulator of clathrin-mediated endocytosis. J. Cell Biol. *156,* 921–929.

Damke, H., Binns, D. D., Ueda, H., Schmid, S. L., and Baba, T. (2001). Dynamin GTPase domain mutants block endocytic vesicle formation at morphologically distinct stages. Mol. Biol. Cell *12,* 2578–2589.

Edeling, M. A., Mishra, S. K., Keyel, P. A., Steinhauser, A. L., Collins, B. M., Roth, R., Heuser, J. E., Owen, D. J., and Traub, L. M. (2006). Molecular switches involving the AP-2 beta2 appendage regulate endocytic cargo selection and clathrin coat assembly. Dev. Cell *10,* 329–342.

Ehrlich, M., Boll, W., Van Oijen, A., Hariharan, R., Chandran, K., Nibert, M. L., and Kirchhausen, T. (2004). Endocytosis by random initiation and stabilization of clathrin-coated pits. Cell *118,* 591–605.

Gaidarov, I., and Keen, J. H. (1999). Phosphoinositide-AP-2 interactions required for targeting to plasma membrane clathrin-coated pits. J. Cell Biol. *146,* 755–764.

Gonzalez-Gaitan, M., and Jackle, H. (1997). Role of *Drosophila* α-adaptin in presynaptic vesicle recycling. Cell *88,* 767–776.

Heuser, J. (1989). Effects of cytoplasmic acidification on clathrin lattice morphology. J. Cell Biol. *108,* 401–411.

Heuser, J. E., and Anderson, R. G. (1989). Hypertonic media inhibit receptor-mediated endocytosis by blocking clathrin-coated pit formation. J. Cell Biol. *108,* 389–400.

Höning, S., Ricotta, D., Krauss, M., Spate, K., Spolaore, B., Motley, A., Robinson, M., Robinson, C., Haucke, V., and Owen, D. J. (2005). Phosphatidylinositol-(4,5)-bisphosphate regulates sorting signal recognition by the clathrin-associated adaptor complex AP2. Mol. Cell *18,* 519–531.

Huang, F., Khvorova, A., Marshall, W., and Sorkin, A. (2004). Analysis of clathrin-mediated endocytosis of epidermal growth factor receptor by RNA interference. J. Biol. Chem. *279,* 16657–16661.

Keyel, P. A., Watkins, S. C., and Traub, L. M. (2004). Endocytic adaptor molecules reveal an endosomal population of clathrin by total internal reflection fluorescence microscopy. J. Biol. Chem. *279,* 13190–13204.

Motley, A., Bright, N. A., Seaman, M.N.J., and Robinson, M. S. (2003). Clathrin-mediated endocytosis in AP-2-depleted cells. J. Cell Biol. *162,* 909–918.

Nesterov, A., Carter, R. E., Sorkina, T., Gill, G. N., and Sorkin, A. (1999). Inhibition of the receptor-binding function of clathrin adaptor protein AP-2 by dominant-negative mutant mu2 subunit and its effects on endocytosis. EMBO J. *18,* 2489–2499.

Olusanya, O., Andrews, P. D., Swedlow, J. R., and Smythe, E. (2001). Phosphorylation of threonine 156 of the mu2 subunit of the AP2 complex is essential for endocytosis in vitro and in vivo. Curr. Biol. *11,* 896–900.

Owen, D. J., Collins, B. M., and Evans, P. R. (2004). Adaptors for clathrin coats: structure and function. Annu. Rev. Cell Dev. Biol. *20,* 153–191.

Owen, D. J., and Evans, P. R. (1998). A structural explanation for the recognition of tyrosine-based endocytic signals. Science *282*, 1327–1332.

Owen, D. J., Vallis, Y., Noble, M. E., Hunter, J. B., Dafforn, T. R., Evans, P. R., and McMahon, H. T. (1999). A structural explanation for the binding of multiple ligands by the alpha-adaptin appendage domain. Cell *97*, 805–815.

Page, L. J., and Robinson, M. S. (1995). Targeting signals and subunit interactions in coated vesicle adaptor complexes. J. Cell Biol. *131*, 619–630.

Rappoport, J. Z., Benmerah, A., and Simon, S. M. (2005). Analysis of the AP-2 adaptor complex and cargo during clathrin-mediated endocytosis. Traffic *6*, 539–547.

Rappoport, J. Z., Taha, B. W., Lemeer, S., Benmerah, A., and Simon, S. M. (2003). The AP-2 complex is excluded from the dynamic population of plasma membrane-associated clathrin. J. Biol. Chem. *278*, 47357–47360.

Ricotta, D., Conner, S. D., Schmid, S. L., von Figura, K., and Höning, S. (2002). Phosphorylation of the AP2 mu subunit by AAK1 mediates high affinity binding to membrane protein sorting signals. J. Cell Biol. *156*, 791–795.

Robinson, M. S. (1993). Assembly and targeting of adaptin chimeras in transfected cells. J. Cell Biol. *123*, 67–77.

Rohde, G., Wenzel, D., and Haucke, V. (2002). A phosphatidylinositol (4,5)-bisphosphate binding site within mu2-adaptin regulates clathrin-mediated endocytosis. J. Cell Biol. *158*, 209–214.

Sambrook, J., and Russell, D. W. (2001). Molecular Cloning, A Laboratory Manual. Cold Spring Harbor, NY: Cold Spring Harbor Laboratory Press.

Simpson, F., Bright, N. A., West, M. A., Newman, L. S., Darnell, R. B., and Robinson, M. S. (1996). A novel adaptor-related protein complex. J. Cell Biol. *133*, 749–760.

Slepnev, V. I., and De Camilli, P. (2000). Accessory factors in clathrin-dependent synaptic vesicle endocytosis. Nat. Rev. Neurosci. *1*, 161–172.

Zacharias, D. A., Violin, J. D., Newton, A. C., and Tsien, R. Y. (2002). Partitioning of lipid-modified monomeric GFPs into membrane microdomains of live cells. Science *296*, 913–916.